FUDMA Journal of Sciences (FJS)
ISSN online: 2616-1370
ISSN print: 2645 - 2944
Vol. 8 No. 5, October, 2024, pp 124 - 133
DOI: https://doi.org/10.33003/fjs-2024-0805-2705

SYNERGISTIC IMPACT OF RICE HUSK ASH AND PULVERIZED CLAY BRICK BLENDS ON CEMENT MORTAR DURABILITY IN MAGNESIUM SULPHATE ENVIRONMENTS

***Isma'il, M., Lawan, A. and Aliyu, I.**

Department of Civil Engineering Ahmadu Bello University, Zaria-Nigeria

*Corresponding authors' email: mukhtarisma92@gmail.com Phone: +2348035357545

ABSTRACT

The use of supplementary cementitious materials (SCMs) in aggressive environments can result in variable performance; while some SCMs enhance pore structure and reduce permeability, others may compromise compressive strength, especially at high replacement levels. This study investigates the potential of rice husk ash (RHA) and pulverized clay brick (PCB) blends as SCMs in magnesium sulphate environments. By leveraging RHA's pozzolanic activity, which enhances strength, and PCB's role in refining pore structure, this research aims to balance strength and durability. RHA-PCB blends (30:70, 40:60, 50:50) were characterized by X-ray fluorescence (XRF) to analyze oxide compositions and synergistic effects, while scanning electron microscopy (SEM) and energy-dispersive X-ray spectroscopy (EDS) provided insights into microstructural and elemental changes due to magnesium sulphate exposure. The Cation Binding Capacity (CBC) of cement, including blends of RHA and PCB, was evaluated to assess the interaction potential of cement mortar with magnesium ions (Mg^{2+}) from magnesium sulphate ($MgSO_4$). Mortar specimens with these blends were cured for 28 days, then immersed in a magnesium sulphate solution for 7, 28, and 56 days. Compressive strengths were measured, and deterioration mechanisms were analyzed. Results indicate that higher PCB content potentially increases interaction with magnesium ions in the $MgSO_4$ solution. However, the 40:60 blend of RHA and PCB, used as a 15% cement replacement, significantly improved durability by enhancing compressive strength while effectively managing the negative effects of magnesium and sulphate ions. This suggests that the 40:60 RHA-PCB blend could be a promising solution for enhancing cement mortar durability in sulphate-rich environments.

Keywords: Cation binding capacity, Rice Husk Ash, Pulverized Clay Brick, Magnesium Sulphate

INTRODUCTION

The construction industry is a major contributor to global greenhouse gas emissions, with cement production alone responsible for up to 9% of these emissions (Marangu et al., 2020). To mitigate this environmental impact, researchers are increasingly exploring sustainable construction materials, including the use of waste products as supplementary cementitious materials (SCMs) (Kaptan et al., 2024). While traditional SCMs like fly ash have been widely studied, there is a growing interest in the potential of various industrial waste materials to enhance concrete durability, particularly in aggressive environments.

Rice husk ash (RHA), which is rich in silica, has been shown to improve concrete strength by forming high-surface-area calcium silicate hydrate (C-S-H) gels during hydration (Charitha et al., 2021). Similarly, pulverized clay brick (PCB), another industrial waste-derived SCM, offers significant benefits. Incorporating PCB into cement not only promotes waste management but also enhances the structural integrity and durability of concrete (Dawood et al., 2021; Msinjili et al., 2021; Sungkono, 2018). Notably, PCB's ability to densify the cement matrix reduces harmful ion infiltration, making it particularly effective in sulfate-rich environments (Hasan et al., 2022; Jhatial et al., 2023).

This study explores the synergistic effects of combining RHA and PCB as partial cement replacements in mortar, with a focus on improving durability in magnesium sulphate environments. By leveraging RHA's strength-enhancing properties and PCB's micro-filler effects, the research aims to mitigate the damaging effects of magnesium sulfate exposure. Magnesium sulfate is known to cause the formation of expansive compounds such as brucite ($Mg(OH)_2$) and gypsum, which can compromise the integrity of cement structures. Sulfate attack is one of the most aggressive environmental factors affecting the long-term durability of cement, and the damage mechanism varies depending on the associated cation (e.g., Na^+, K^+, Mg^{2+}, Ca^{2+}). Specifically, magnesium cations (Mg^{2+}) in $MgSO_4$ can act as catalysts or directly contribute to degradation (Müllauer et al., 2013; Neville, 2004; Santhanam et al., 2003). PCB, despite its pozzolanic properties, contains clay minerals with highly negatively charged surfaces that attract and bind cations, which can be either beneficial or detrimental depending on the cations present (Mousavi et al., 2021).

Previous research, such as that by Marangu et al. (2024), has demonstrated the effectiveness of simultaneously substituting RHA and calcined clay (CC) to improve concrete durability. However, the synergistic effects of combining RHA and PCB as a single SCM, particularly their interaction with magnesium (Mg^{2+}) and sulphate ions (SO_4^{2-}) in magnesium sulfate environments, remain underexplored. For example, Gill and Sadique, (2018) reported a decrease in compressive strength in self-compacting concrete (SCC) with ternary blends of RHA and metakaolin (MK) after 28 days of curing in a sulphate environment, though the addition of 10% RHA and 10% MK showed improved performance compared to other blends. Despite the potential benefits of combining two waste materials as a single SCM, further investigation into their synergistic effects is needed.

This study aims to identify a blending ratios of RHA and PCB that maximizes their beneficial properties. Various blend ratios (30:70, 40:60, and 50:50) of RHA to PCB were used to replace cement at different levels (0%, 5%, 10%, 15%, and 20%) to determine the best combination for enhancing the overall durability of cement mortar in aggressive environments with high magnesium sulphate content.

MATERIALS AND METHODS

Materials

Recycled clay brick were derived from brick remnants collected from a production facility at the Industrial Development Centre (IDC) in Samaru, Zaria. Rice husk, a by-product of rice milling processes in Zaria, was processed to obtain rice husk ash.

Fine Aggregates

The research utilized naturally occurring, clean, and well-graded sands, sourced from Zaria, which are recognized for their suitability in concrete and mortar formulations.

Cement

Portland Limestone Cement (PLC), Dangote brand, Grade 42.5N, was used.

Water

Clean, potable water sourced from the Concrete and Materials Laboratory at the Department of Civil Engineering, Ahmadu Bello University, Zaria, was used for preparing the mortar samples.

Methods

Preparations of Samples

Preparation of Rice Husk Ash

Rice husk ash (RHA) was produced by initially burning rice husks in an open air burning chamber, the husk was sieved using 75μmm sieve and subsequently calcined at 500°C for one hour in a muffle furnace. This temperature was chosen to maximize silica yield based on recommendation of Hindarso et al., (2021).

Preparation of Pulverized Clay Brick (PCB)

Pulverized clay brick (PCB) was prepared by grinding and refining broken bricks from construction and factory sites using a pulverizing machine at Geology department Ahmadu Bello University Zaria.

Preparation of RHA-PCB blends and Cement Replacement

The study utilized Portland Limestone Cement with grade 42.5N, substituting it with the RHA-PCB blend at replacement levels of 0%, 5%, 10%, 15%, and 20%. Each level of cement replacement featured the blend of RHA-PCB at a combining ratio of 30% RHA and 70% PCB, 40% RHA and 60% PCB, and 50% RHA and 50% PCB respectively. A mechanical blending process, lasting for equal duration for all the blends, ensured a uniformly mixed blend.

Experimental Procedures

Material Characterization

X-ray fluorescence (XRF) analysis was conducted to determine the oxide composition of RHA, PCB, and their blends (30:70, 40:60, and 50:50). This analysis is important for assessing the potential of these materials as supplementary cementitious materials (SCMs).

Cation Binding Capacity Test

The CBC test was conducted adhering to the ASTM D7503 – 10 guidelines to evaluates the blends potential interaction with the magnesium ion (mg^{2+}) in the magnesium sulphate solution, employing the ammonium acetate method at a neutral pH, as this is the most widely utilized approach for determining CBC. A sample amount of 10 grams was placed in a 100-milliliter centrifuge tube with 40 milliliters of 1 M ammonium acetate (pH 7) and shaken for 5 minutes. The tube was left overnight and shaken for an additional 15 minutes the next day. The sample was filtered through a Buchner funnel into a vacuum flask, and the remaining sample in the tube was rinsed. The sample was washed four times with 30 milliliters of ammonium acetate, then three times with 40 milliliters of isopropanol, and finally four times with 50 milliliters of potassium chloride solution. The solution from the vacuum flask was transferred to a volumetric flask (250 milliliters), and 60 milliliters were extracted for nitrogen concentration determination using a spectrophotometer. The nitrogen concentration was used to calculate the cation binding capacity. The test was conducted on the constituent materials—cement (OPC) and cement mixed with various RHA-PCB blends (30:70, 40:60, and 50:50) at replacement levels of 5%, 10%, 15%, and 20%. These tests were performed at the Department of Soil Science, Ahmadu Bello University, Zaria.

Physical Properties of Cement and Fine aggregates

Test on aggregates were carried out in accordance with guidelines specified in **BS 882, Part 2.** The physical properties of the cement paste, including consistency, setting times, and soundness, were examined in accordance with BS EN 196-3 (1995) standards.

Determination of Loss on Ignition (LoI)

For LoI determination, samples were weighed and placed in porcelain crucibles. The weight of the empty crucible (W1) and the crucible with the sample (W2) were recorded. Samples were heated in a muffle furnace at 900°C for 30 minutes. Post-cooling, the final weight (W3) was measured. LoI was calculated as the percentage loss in mass from the original sample post-heating. The test was also carried out at the Department of Soil Science, Ahmadu Bello University Zaria.

Preparation of Magnesium Sulphate Solution

Magnesium sulphate ($MgSO_4$) solution was prepared meeting the ASTM C 1012-04 standard of 50 g/L with pH of 6.3.

Curing of Mortar Samples and Exposure to Sulphate Solution

Mortar specimens of size 50mmx50mmx50mm containing various blends (30:70, 40:60 and 50:50) of RHA to PCB were initially cured in water for 28 days then transferred to a magnesium sulphate ($MgSO_4$) solution for varying durations: 7, 28, and 56 days. In addition, a separate group of samples remained in water and were not exposed to the $MgSO_4$ solution. These unexposed samples were crushed at the same time points as the exposed samples, acting as reference points for strength comparisons at the end of each exposure period.

RESULTS AND DISCUSSION

Material Characterization

The oxide composition test was carried out on the RHA, PCB and the various blends of RHA-PCB using the X-ray florescence (XRF). The results of the analysis are presented in table 1.

Table 1: Oxide Composition test results

OXIDES	**RHA**	**PCB**	**RHA+PCB (50:50)**	**RHA+PCB (40:60)**	**RHA+PCB (30:70)**
SiO_2	64.39	48.27	61.19	62.41	58.84
Al_2O_3	3.83	18.54	6.96	10.48	12.81
Fe_2O_3	4.60	19.09	12.73	9.23	10.35
SO_3	1.82	0.31	1.03	1.16	1.100
MgO	0.00	0.00	0.00	0.00	0.00
Cl	2.11	1.07	1.13	0.84	0.82
K_2O	12.61	4.70	7.67	5.17	4.80
CaO	8.59	4.50	5.26	3.67	3.51
$SiO_2+Al_2O_3+Fe_2O_3$	72.82	85.90	80.88	82.12	82.00
LOI	14.50	1.20	8.60	6.80	6.00

The silica (SiO_2) content in RHA was 64.39%, higher than PCB's 48.27%, but slightly lower than the 68.12% reported by Dabai et al. (2010). When RHA was blended with PCB at different ratios (30:70, 40:60, and 50:50), some inconsistencies in SiO_2 content were observed, with the 40:60 blend showing the highest SiO_2 concentration. These inconsistencies may be due to the blending methods used, which might not have fully achieved homogeneity across the blends. This suggests that the blending process could be refined in future studies to produce more consistent oxide distributions. Importantly, the RHA, PCB, and all the blends met the ASTM C-168-19 (2019) requirements for primary oxides.

According to ASTM C-168-19 (2019) regulatory standards, the Loss on Ignition (LoI) should not exceed 12%. The PCB and various RHA-PCB blends, all comply with these standards. However, the LoI of the RHA exceeded the maximum threshold stipulated by ASTM C-168-19 (2019). The elevated LoI observed in RHA is likely due to unburned organic matter, but this decreases with higher PCB proportions, illustrating the impact of blending the two materials and processing conditions on the final properties.

Soundness Test Result of Cement Containing the Various Blends of RHA-PCB as Partial Replacements

Figure 1 presents the results of the soundness test for cement partially replaced with RHA-PCB blends. The soundness results for the various RHA-PCB blends (30:70, 40:60, and 50:50) and cement replacement levels (5%, 10%, 15%, and 20%) revealed consistent trends across the different combinations. Importantly, all soundness values for these blends fell within the acceptable range of 0-10 mm, as specified by BS EN 196-3 (1995), which defines cement as unsound if the value exceeds 10 mm (Sulaiman and Aliyu, 2020). For the 30:70 and 50:50 blends, soundness initially decreased as the replacement level increased, but a slight increase was observed at the 15% replacement level. In contrast, the 40:60 blend exhibited an increase in soundness as the RHA-PCB content rose from 5% to 15%, followed by a decrease at the 20% replacement level. These variations suggest that the interaction between RHA, PCB, and cement at specific replacement levels can induce microstructural changes that may influence expansion.

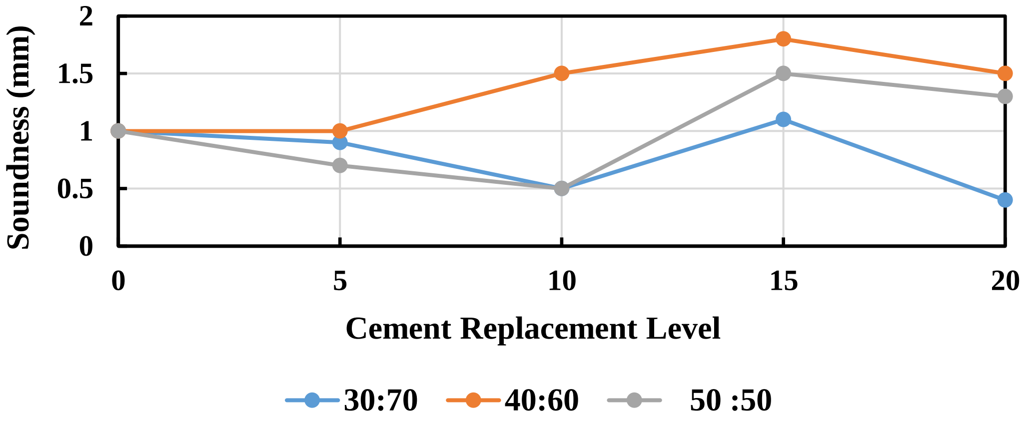

Figure 1: Chart showing the soundness of cement at different level of RHA/PCB replacement

Result of Consistency of Cement-paste Containing RHA-PCB

The investigation into the water demand for achieving normal consistency reveals a direct correlation with the level of cement replacement by the RHA-PCB blend, as seen in Figure 2. Specifically, as the proportion of the RHA-PCB blend increases, there is a consequent rise in water demand to reach the desired consistency. This means that as the content of RHA-PCB increases in the cement paste, the required plasticity is achieved with increased water content. The same behaviour was observed by Aliyu et al. (2020) in cement mortar containing PCB.

When comparing the RHA-PCB blends to the control (100% PLC), it was observed that the control required less water to achieve normal consistency compared to the blended cements. This is because a higher quantity of water is required to wet the RHA-PCB particles added to the cement, similar to the observation made by Sulaiman and Aliyu, (2020) on RHA/Cement Kiln Dust (CKD) as cement replacement material. This trend is further accentuated within the various RHA-PCB blends, where an increase in RHA from 30%

(30:70 blend) to 40% (40:60 blend) and 50% (50:50 blend) results in a greater water requirement. The increased water demand in these blends can be attributed to the smaller particle sizes of RHA, which increase the surface area of the blend, thus requiring more water for normal consistency. These findings align with the observations and conclusions drawn in prior studies by Assumptor et al. (2020) and Endale et al. (2022), highlighting the consistency of these outcomes across different research efforts.

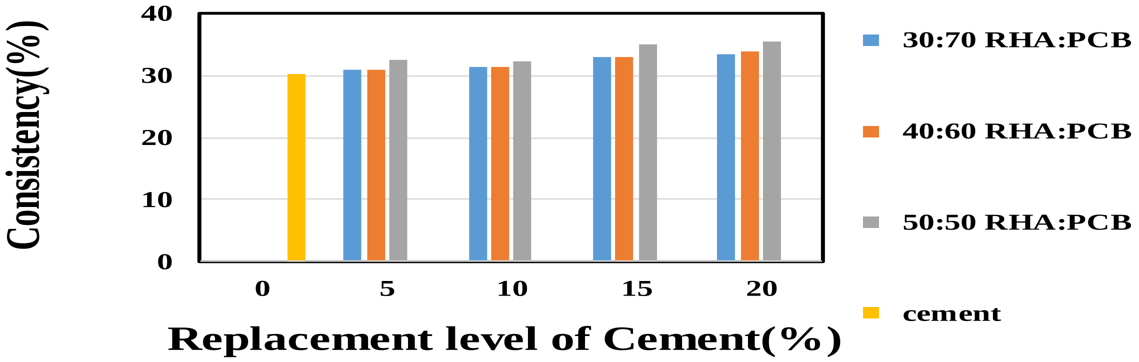

Figure 2: Consistency test for cement and all the mixes of RHA-PCB at different level of cement replacement

Change in Weight of Mortar Samples Containing Various Blends of RHA-PCB Exposed to Magnesium Sulphate

The weight change measurements for cement mortars containing different RHA-PCB blends (30:70, 40:60, and 50:50) after curing for 28 days and subsequent exposure to magnesium sulphate ($MgSO_4$) for 7, 28, and 56 days are shown in Figure 3. These results provide insights into the durability of the blends under sulphate attack.

The 30:70 blend exhibited a consistent increase in weight across all replacement levels. At 0% cement replacement, the weight change increased from 0.41% after 7 days to 0.72% after 56 days, with the highest weight gain of 0.89% at the 15% replacement level. This steady increase suggests moderate susceptibility to magnesium sulphate, likely due to the formation of expansive compounds such as ettringite.

The 40:60 blend showed a different pattern, with weight change increasing significantly as the replacement level rose from 5% to 15%. The maximum weight change was 0.84% at the 15% replacement level after 56 days, indicating that this blend may be more vulnerable to sulphate attack, particularly at higher replacement levels, due to greater expansion from expansive compound formation.

The 50:50 blend demonstrated a relatively steady increase in weight over time, starting at 0.41% after 7 days at 0% replacement. The highest weight gain of 0.81% was observed at the 10% replacement level after 56 days. This suggests that while the 50:50 blend is also affected by sulphate exposure, it may offer a more balanced resistance to expansion compared to the other blends.

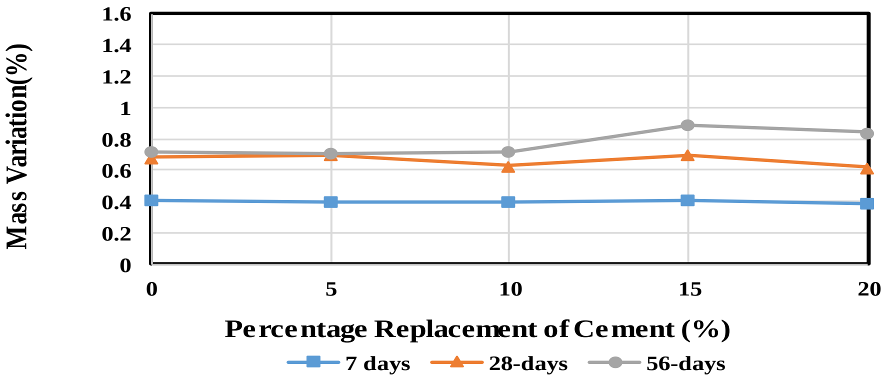

(a) **30:70**

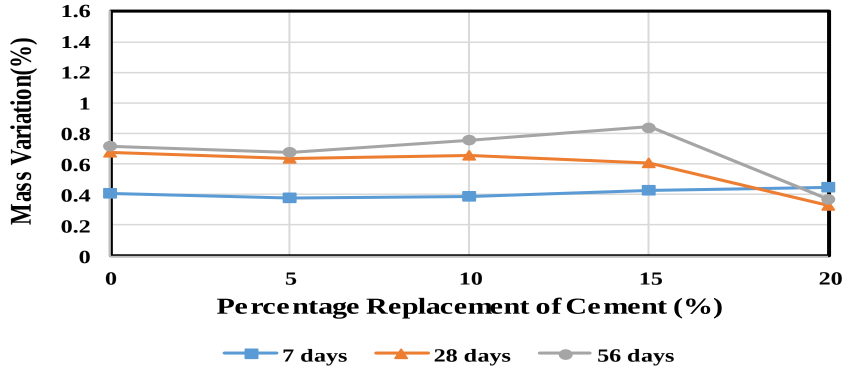

(b) 40:60

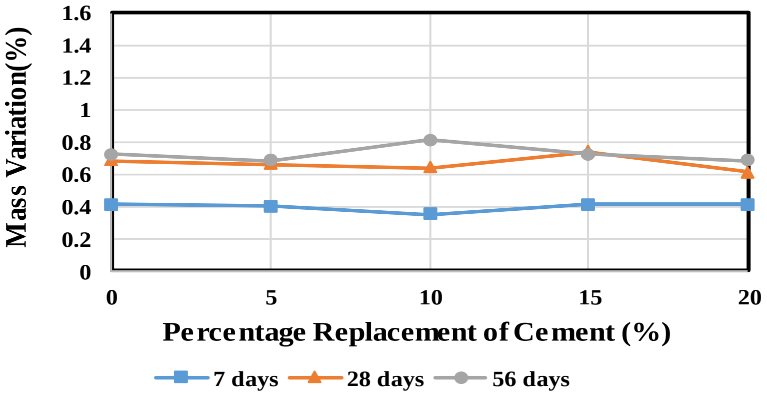

(c) 50:50

Figure 3: Change in weight of samples cured for 28 days, then exposed to magnesium sulphate for 7, 28, 56 days

Compressive Strength of Mortar Samples Containing Various Blends of RHA-PCB Exposed to Magnesium Sulphate

Figure 4 illustrates the compressive strength of samples with various RHA-PCB blends, cured for 28 days and then exposed to magnesium sulfate for 7, 28, and 56 days. It can be seen that, at 15% cement replacement, all the blended samples demonstrated higher compressive strength than the 100% PLC mortar samples after 56 days of magnesium sulfate exposure. This improved performance is likely due to the completion of the pozzolanic reaction of both RHA and PCB at the later exposure period (Marangu et al., 2020). Notably, the samples with the 40:60 blend achieved the highest compressive strength of 19.47 N/mm² at 15% cement replacement after 56 days in magnesium sulphate, followed by the 50:50 blend with 17.07 N/mm², and the 30:70 blend with 13.33 N/mm² compressive strength.

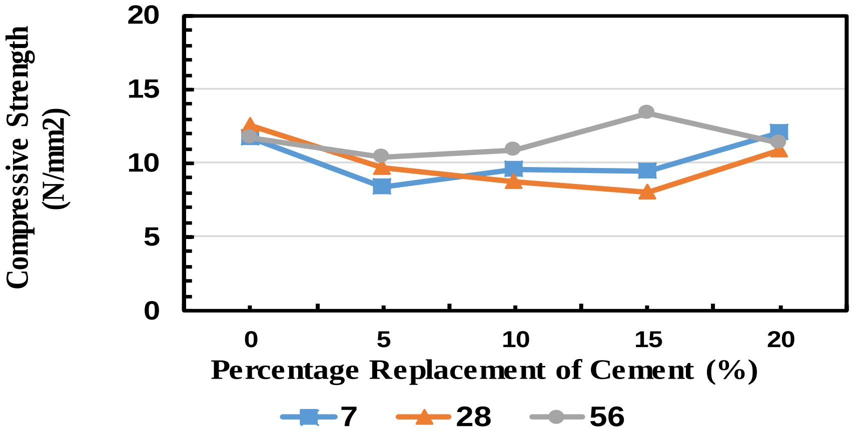

(a) 30:70

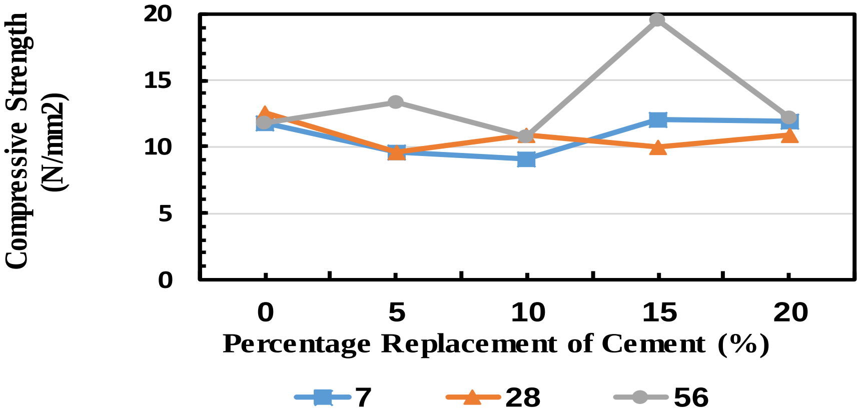

(b) 40:60

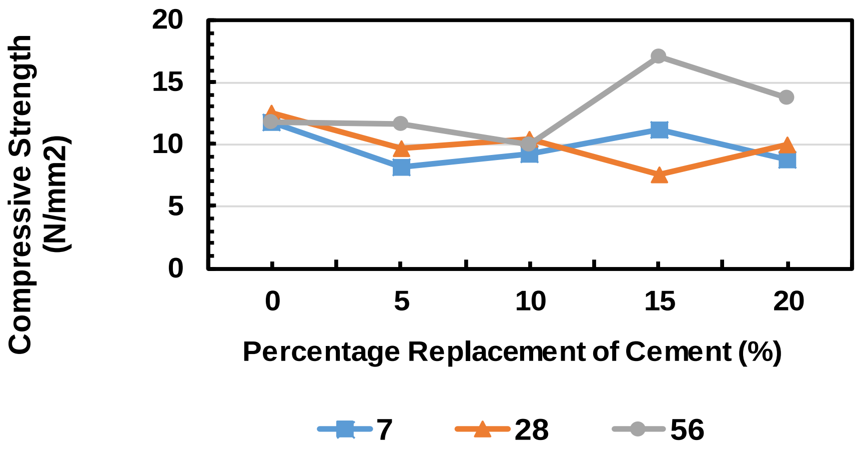

(c) 50:50

Figure 4: Compressive strength of mortar samples containing various RHA-PCB blends, exposed to magnesium sulfate for 7, 28, and 56 days

Comparison of the Performances of Mortar Samples Containing the RHA-PCB blends After Exposure to Magnesium Sulphate

Figure 5 compares the performance of different RHA-PCB blends after a 56-day exposure period. From the chart, it can be seen that all blends demonstrated improved strength at 15% cement replacement, with the 40:60 blend achieving the highest strength, followed by the 50:50 and 30:70 blends. This improved performance is likely due to the high reactivity of the RHA blends at the 15% replacement level, as reported by Marangu et al, (2020)

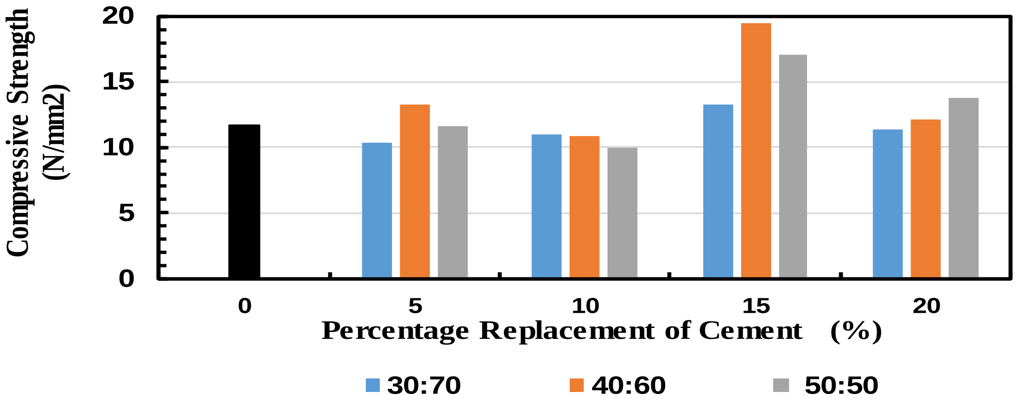

Figure 5: Comparison of compressive strength of mortar samples containing various blends of RHA-PCB after 56 days of exposure to magnesium sulfate

Effects of Magnesium Sulphate on Mortar Samples Containing the Blends of RHA-PCB

Figure 6 shows the compressive strength of samples cured for 28 days and then exposed to magnesium sulfate for 7, 28, and 56 days, along with their corresponding control samples (cured only in water). The control samples generally exhibited higher strength than the exposed samples. However, the samples with the 40:60 blend at 15% cement replacement level exhibited higher compressive strength than their control after 56 days of exposure to magnesium sulfate. This behavior may be due to the high infiltration of sulfate ions into the mortar samples, which filled pore spaces due to initial precipitation of expansive compounds and temporarily increased strength higher than their corresponding controls, this behavior is similar to the observations made by Li et al, (2022).

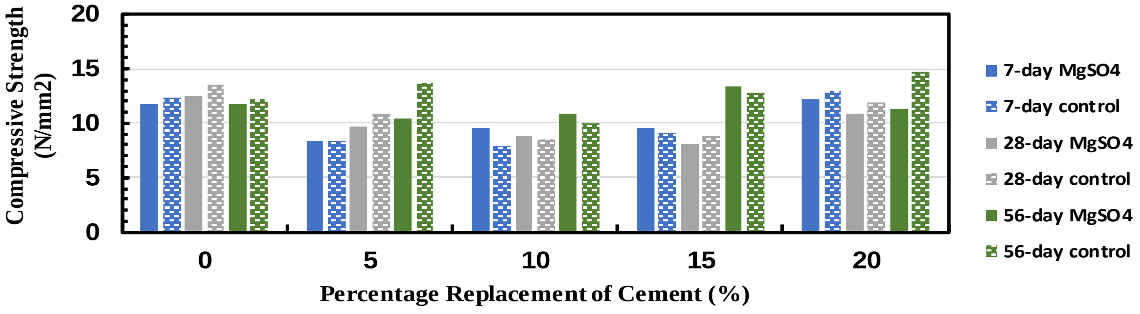

(a) 30:70

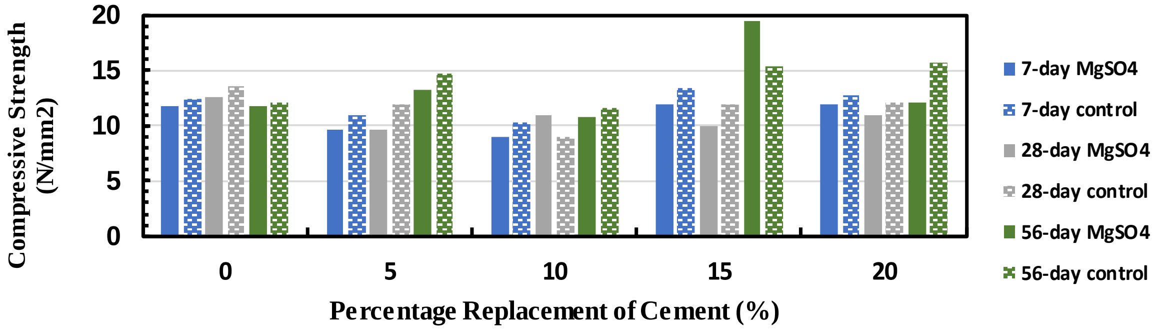

(b) 40:60

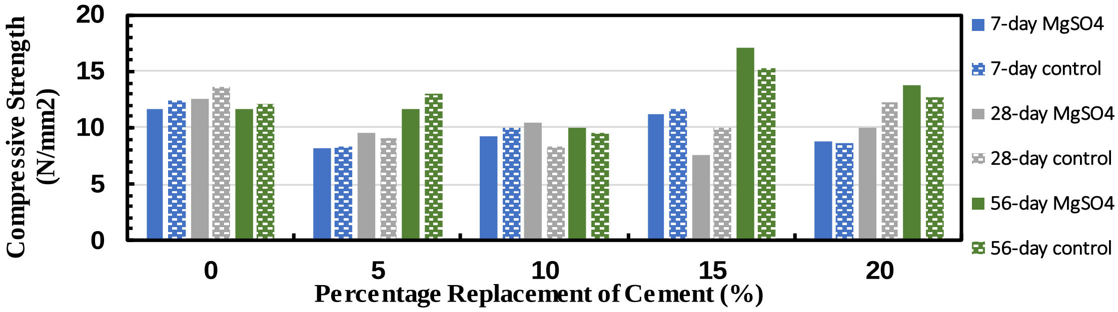

(c) 50:50

Figure 6: Compressive Strength Comparison of Samples Cured for 28 Days then Exposed to Magnesium Sulfate for 7, 28, and 56 Days with Water-Cured Controls

Elemental and Morphological Analysis of Cement Mortar Containing RHA-PCB after Magnesium Sulphate Exposure

This section presents microstructural and elemental analyses of mortar samples containing varying RHA-PCB blend ratios (30:70, 40:60, and 50:50) at a 15% cement replacement level, alongside a control sample (100% PLC) exposed to magnesium sulphate for 56 days. Table 2 summarizes the elemental composition of the samples supporting these findings. Control samples made with 100% Portland Limestone Cement (PLC) became denser after 56 days of exposure to magnesium sulfate as can be seen in figure 7. This densification is due to the high content of CaO and silicon dioxide (SiO_2), along with moderate amounts of iron oxide (Fe_2O_3) and aluminum oxide (Al_2O_3), which help strengthen and densify the mortar (Adhikary et al., 2022).

The 40:60 blend (40% RHA and 60% PCB) was the most porous as seen in figure 9. The higher porosity of the 40:60 blends compared to other blends may primarily be to due pozzolanic effect of the blend due to its higher silicon oxide content as seen in table 1, leading to the formation of additional hydrates (Marangu et al., 2020). The high sulfur (S) content of this blend indicates significant sulphate infiltration, which may be responsible for the strength development of samples containing the blends, due to initial precipitation of expansive compounds.

The 30:70 blend (30% RHA and 70% PCB) was less porous than the 40:60 blend as seen in figure 8. This reduction in porosity might be due to the increased PCB content, as clay particles in RHA has been reported to decrease the values of open pores, contributing to microstructure development (Marangu et al., 2020). This blend showed lower sulphate ion infiltration, indicated by its lower sulfur content as seen in table 2.

The 50:50 blend (equal parts RHA and PCB) was the densest among all samples as seen in figure 10. This is likely due to its higher CaO content as indicated in table 1 and 2. The high CaO content supports the formation of additional C-S-H, forming a denser structure, resulting in less sulphate intrusion and greater long-term durability.

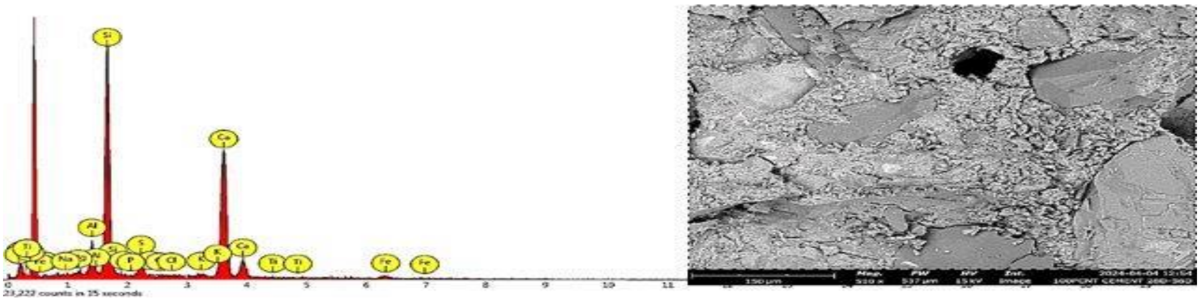

Figure 7: EDX and SEM images of Control sample (100% PLC) exposed to magnesium sulphate for 56 days

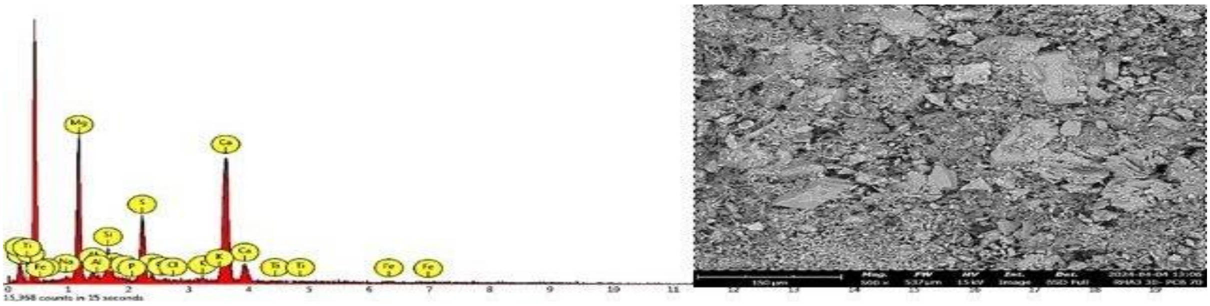

Figure 8: EDX and SEM images of sample containing 30:70 blends (30% RHA and 70% PCB) exposed to magnesium sulphate for 56 days

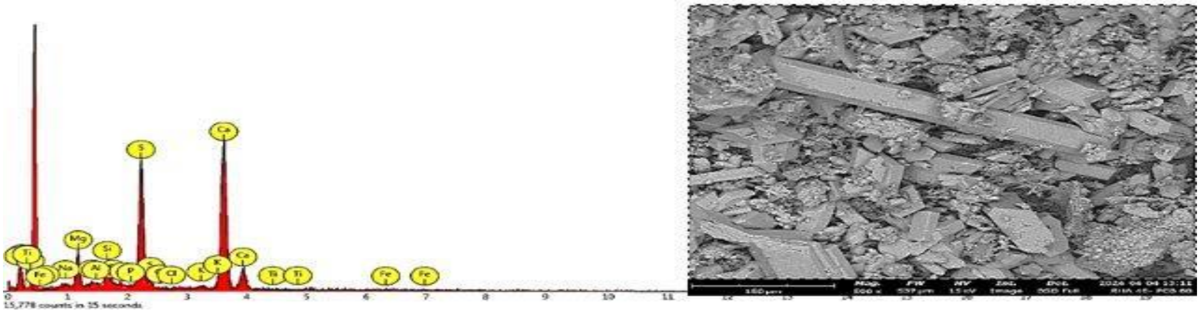

Figure 9: EDX and SEM images of sample containing 40:60 blends (40%RHA and 60% PCB) exposed to magnesium sulphate for 56 days

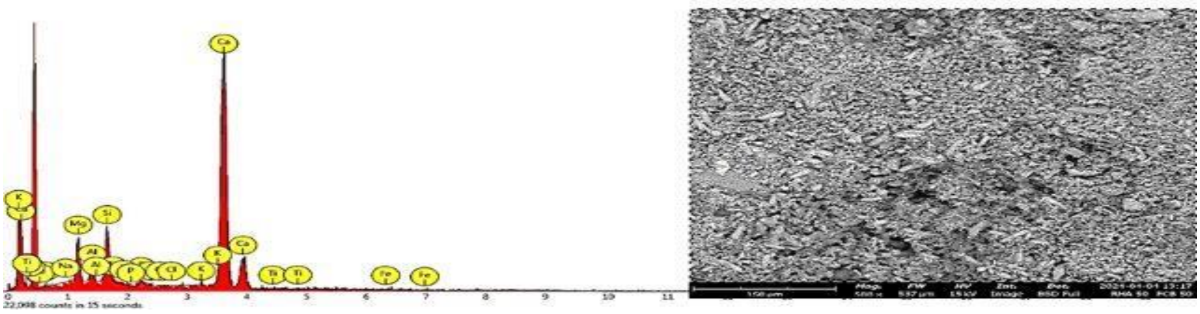

Figure 10: EDX and SEM images of sample containing 50:50 blends (equal parts RHA and PCB) exposed to magnesium sulphate for 56 days

Table 2: Summary of EDX results showing elemental compositions of samples exposed to magnesium sulphate for 56 days

Element Name	**Weight Concentration**			
	OPC	**30:70**	**40:60**	**50:50**
Calcium (Ca)	49.39	49.44	60.60	79.07
Silicon(Si)	38.05	5.61	8.91	3.48
Aluminum(Al)	5.39	1.97	0.41	2.45
Sulfur(S)	4.32	14.51	27.23	1.10
Iron (Fe)	2.03	1.48	0.00	0.63
Potassium(K)	0.43	0.65	1.05	0.00
Magnesium(Mg)	0.40	25.58	6.57	7.84
Sodium(Na)	0.00	0.54	0.35	0.00
Titanium(Ti)	0.00	0.00	0.00	0.00
Phosphorus(P)	0.00	0.22	0.00	0.00
Chlorine(Cl)	0.00	0.00	0.30	0.00

Potential Effects of the Cation Binding Capacity (CBC) on the Strength and Durability of the Cement-RHA-PCB mortar samples

The cation binding capacity (CBC) of cement, partially replaced with various blends of RHA-PCB was evaluated to determine their potential interaction with magnesium ions (Mg^{2+}) from magnesium sulfate solution. And the result is presented in figure 11. The control sample (cement) has a CBC of 24.10 C-mole/kg as seen in figure 11, indicating a moderate capacity to interact with magnesium ions, forming stable compounds that enhance mortar density.

The 30:70 blend exhibited the highest CBC of 26.20 C-mole/kg, leading to the highest magnesium content (25.58 mg/g). This strong interaction promotes the formation of stable but expansive compounds like $Mg(OH)_2$, which initially fill voids in the mortar but can cause micro-cracking over time, compromising long-term durability.

The 40:60 blend, with a CBC of 24.70 C-mole/kg, showed similar potential interaction to the control, allowing effective magnesium ion binding without excessive formation of expansive compounds. Its magnesium content is 6.57 mg/g, indicating moderate $Mg(OH)_2$ formation. However, its porous structure allowed significant sulphate intrusion, increasing vulnerability to sulfate attack.

The 50:50 blend had a CBC of 24.6 C-mole/kg and a magnesium content of 7.84 mg/g, suggesting moderate $Mg(OH)_2$ formation. The higher calcium content facilitated additional C-S-H formation, resulting in a denser structure with reduced sulphate intrusion. This blend also demonstrated potential long-term durability, indicating the need for further investigation with extended exposure to magnesium sulphate beyond 56 days.

The results also indicate that higher PCB content in the blend increases the potential interaction with Mg^{2+} to form expansive compounds like $Mg(OH)_2$. This behavior is likely due to the high cation binding capacity of clay minerals, which have negatively charged surfaces that attract positively charged ions (Mousavi et al., 2021).

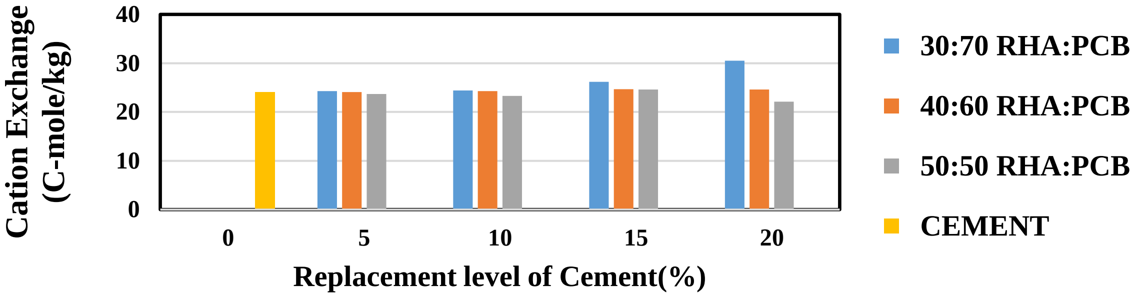

Figure 11: Cation binding capacity of cement partially replaced with various blends of RHA-PCB

CONCLUSION

XRF analysis confirmed that combining RHA with PCB significantly alters the oxide composition of the blend, increasing the content of primary oxides essential for pozzolanic activity. The study revealed that samples containing 30:70, 40:60, and 50:50 RHA-PCB blends exhibited higher compressive strength than the control (100% PLC) after 56 days of exposure to magnesium sulfate at a 15% cement replacement level. Among these, the 40:60 blend achieved the highest compressive strength of 19.47 N/mm^2. However, the elevated sulphur content in the blend may increase susceptibility to sulphate attack beyond 56 days of exposure.

The 50:50 blend demonstrated the densest morphology, resulting in minimal infiltration of magnesium and sulphate ions, potentially offering superior long-term durability compared to the other blends. Additionally, the study found that increased PCB content in the samples correlated with a higher interaction potential with Mg^{2+} in the magnesium sulphate solution. The 50:50 blend, in particular, exhibited moderate interactions with both sulphates and magnesium ions, reducing the formation of expansive compounds like magnesium hydroxide ($Mg(OH)_2$) and ettringite in high-magnesium sulphate environments.

In conclusion, this study has demonstrated the effectiveness of a 40:60 blend of Rice Husk Ash and Pulverized Clay Brick at 15% as a supplementary cementitious material for enhancing cement mortar durability in magnesium sulphate environments. The observed synergistic effects provide a sustainable and cost-effective solution for construction in sulphate-rich areas. Future research should explore the long-term performance of these blends and their applicability across various environmental conditions.

REFERENCES

Abiodun, Y. O., & Jimoh, A. A. (2018). Microstructural characterisation, physical and chemical properties of rice husk ash as viable Pozzolan in building material: A case study of some Nigerian grown rice varieties. *Nigerian Journal of Technology*, *37*(1), 71. https://doi.org/10.4314/njt.v37i1.10

Adhikary, S. K., Ashish, D. K., & Rudžionis, Ž. (2022). A review on sustainable use of agricultural straw and husk biomass ashes: Transitioning towards low carbon economy. *Science of The Total Environment*, *838*, 156407. https://doi.org/10.1016/j.scitotenv.2022.156407

Aliyu, I., Tasiu, A. S., Muhammad, A., & Ismail, M. (2020). Effect of Magnesium Sulphate on Calcined Clay Brick Powder Cement Replaced Mortar. *JOURNAL OF SCIENCE TECHNOLOGY AND EDUCATION 8(2), JUNE, 2020, 8(2),* 131.

Assumptor, O. M., Masika, E., & Thiong'o, K. (n.d.). *Probing Optimal Blends of Pozzolans to Develop Supplementary Cementing Material Within Busia County, Kenya.*

ASTM C-168-19 (2019). Standard Specification for Coal Fly Ash and Raw or Calcined Natural Pozzolan for Use in Concrete. West Conshohocken, PA: American Society for Testing and Materials (ASTM) International. Retrieved from www.astm.org.

ASTM C 1012-04 (2004). Standard test Method for Length Change of Hydraulic-Cement Mortars Exposed to a Sulfate Solution. West Conshohocken, PA: American Society for Testing and Materials (ASTM) International.

ASTM D7503 – 10. (July 1, 2010). Standard Test Method for Measuring the Exchange Complex and Cation Exchange Capacity (CEC) of Inorganic Fine-Grained Soils.

BS 882, Part 2, (1992). Grading limits for fine aggregates, British Standard Institution, London.

BS EN 196, Part 3, (1995). Methods of testing cement: Determination of setting time and soundness. British Standard Institution, London.

Charitha, V., Athira, V. S., Jittin, V., Bahurudeen, A., & Nanthagopalan, P. (2021). Use of different agro-waste ashes in concrete for effective upcycling of locally available resources. *Construction and Building Materials*, *285*, 122851. https://doi.org/10.1016/j.conbuildmat.2021.122851

Dabai, M., Muhammad, C., Bagudo, B., & Musa, A. (2010). Studies on the Effect of Rice Husk Ash as Cement Admixture. *Nigerian Journal of Basic and Applied Sciences*, *17*(2), 252–256. https://doi.org/10.4314/njbas.v17i2.49917

Dawood, A. O., Mussa, F. I., Khazraji, H. A., Ulsada, H. A. A., & Yasser, M. M. (2021). Investigation of Compressive Strength of Straw Reinforced Unfired Clay Bricks For Sustainable Building Construction. *Civil and Environmental Engineering*, *17*(1), 150–163. https://doi.org/10.2478/cee-2021-0016

Endale, S. A., Taffese, W. Z., Vo, D.-H., & Yehualaw, M. D. (2022). Rice Husk Ash in Concrete. *Sustainability*, *15*(1), 137. https://doi.org/10.3390/su15010137

Gill, A. S., & Siddique, R. (2017). Strength and micro-structural properties of self-compacting concrete containing metakaolin and rice husk ash. *Construction and Building Materials*, *157*, 51–64. https://doi.org/10.1016/j.conbuildmat.2017.09.088

Hasan, N. Md. S., Sobuz, Md. H. R., Khan, Md. M. H., Mim, N. J., Meraz, Md. M., Datta, S. D., Rana, Md. J., Saha, A., Akid, A. S. M., Mehedi, Md. T., Houda, M., & Sutan, N. M. (2022). Integration of Rice Husk Ash as Supplementary Cementitious Material in the Production of Sustainable High-Strength Concrete. *Materials*, *15*(22), 8171. https://doi.org/10.3390/ma15228171

Hindarso, H., Epriliati, I., Hoerudin, D., & Yuliani, S. (2021). Synthesis and Characterization of Biosilica from Rice Husks as a Catalyst for the Production of Biodiesel. *Fine Chemical Engineering*, 41–46. https://doi.org/10.37256/fce.222021735

Jhatial, A. A., Nováková, I., & Gjerløw, E. (2023). A Review on Emerging Cementitious Materials, Reactivity Evaluation and Treatment Methods. *Buildings*, *13*(2), 526. https://doi.org/10.3390/buildings13020526

Kaptan, K., Cunha, S., & Aguiar, J. (2024). A Review: Construction and Demolition Waste as a Novel Source for CO2 Reduction in Portland Cement Production for Concrete. *Sustainability*, *16*(2), 585. https://doi.org/10.3390/su16020585

Li, X., Yu, X., Zhao, Y., Yu, X., Li, C., & Chen, D. (2022). Effect of initial curing period on the behavior of mortar under sulfate attack. *Construction and Building Materials*, *326*, 126852. https://doi.org/10.1016/j.conbuildmat.2022.126852

Marangu, J. M., Muturia M'thiruaine, C., & Bediako, M. (2020). Physicochemical Properties of Hydrated Portland Cement Blended with Rice Husk Ash. *Journal of Chemistry*, *2020*, 1–10. https://doi.org/10.1155/2020/5304745

Mousavi, S. S., Bhojaraju, C., & Ouellet-Plamondon, C. (2021). Clay as a Sustainable Binder for Concrete—A Review. *Construction Materials*, *1*(3), 134–168. https://doi.org/10.3390/constrmater1030010

Msinjili, N. S., Vogler, N., Sturm, P., Neubert, M., Schröder, H.-J., Kühne, H.-C., Hünger, K.-J., & Gluth, G. J. G. (2021). Calcined brick clays and mixed clays as supplementary cementitious materials: Effects on the performance of blended cement mortars. *Construction and Building Materials*, *266*, 120990. https://doi.org/10.1016/j.conbuildmat.2020.120990

Müllauer, W., Beddoe, R. E., & Heinz, D. (2013). Sulfate attack expansion mechanisms. *Cement and Concrete Research*, *52*, 208–215. https://doi.org/10.1016/j.cemconres.2013.07.005

Neville, A. (2004). The confused world of sulfate attack on concrete. *Cement and Concrete Research*, *34*(8), 1275–1296. https://doi.org/10.1016/j.cemconres.2004.04.004

Santhanam, M., Cohen, M. D., & Olek, J. (2003). Mechanism of sulfate attack: A fresh look. *Cement and Concrete Research*, *33*(3), 341–346. https://doi.org/10.1016/S0008-8846(02)00958-4

Sulaiman, T. A., & Aliyu, I. (2020). Combined Effect of Rice Husk Ash and Cement Kiln Dust as Cement Replacement Materials in Concrete. *Fudma Journal of Sciences*, *4*(1), 446 - 452. Retrieved from https://fjs.fudutsinma.edu.ng/index.php/fjs/article/view/66

Sungkono, K. (2018). Characteristics Of Clay Tile With Rice Husk Ash On Absorption And Flexural Strength. *Proceedings of the The 1st International Conference on Computer Science and Engineering Technology Universitas Muria Kudus*. The 1st International Conference on Computer Science and Engineering Technology Universitas Muria Kudus, Kudus, Indonesia. https://doi.org/10.4108/eai.24-10-2018.2280589